AIP Journal of Applied Physics

The role of Ge-related oxygen-deficiency centers in controlling the blue-violet photo- and electroluminescence in Ge-rich SiO 2 via Er doping

A. Kanjilal, S. Tsushima, C. Götz, L. Rebohle, M. Voelskow, W. Skorupa, and M. Helm

Citation: Journal of Applied Physics **106**, 063112 (2009); doi: 10.1063/1.3225911
View online: http://dx.doi.org/10.1063/1.3225911
View Table of Contents: http://scitation.aip.org/content/aip/journal/jap/106/6?ver=pdfcov
Published by the AIP Publishing

Articles you may be interested in
Controlling blue-violet electroluminescence of Ge-rich Er-doped SiO 2 layers by millisecond annealing using flash lamps
J. Appl. Phys. **107**, 023114 (2010); 10.1063/1.3296252

Defect-engineered blue-violet electroluminescence from Ge nanocrystal rich SiO 2 layers by Er doping
J. Appl. Phys. **106**, 026104 (2009); 10.1063/1.3183904

Bright upconversion white light emission in transparent glass ceramic embedding Tm 3 + Er 3 + Yb 3 + : - Y F 3 nanocrystals
Appl. Phys. Lett. **91**, 251903 (2007); 10.1063/1.2825285

Luminescence and visible upconversion in nanocrystalline ZrO 2 : Er 3+
Appl. Phys. Lett. **83**, 4903 (2003); 10.1063/1.1632020

1.54 m Er 3+ photoluminescent properties of erbium-doped Si/SiO 2 superlattices
Appl. Phys. Lett. **74**, 1573 (1999); 10.1063/1.123620

Journal of Applied Physics is pleased to announce André Anders as its new Editor-in-Chief

[This article is copyrighted as indicated in the article. Reuse of AIP content is subject to the terms at: http://scitation.aip.org/termsconditions. Downloaded to] IP: 131.217.6.8 On: Wed, 03 Sep 2014 10:25:56

The role of Ge-related oxygen-deficiency centers in controlling the blue-violet photo- and electroluminescence in Ge-rich SiO_2 via Er doping

A. Kanjilal,[1,a)] S. Tsushima,[2] C. Götz,[2] L. Rebohle,[1] M. Voelskow,[1] W. Skorupa,[1] and M. Helm[1]

[1]*Institute of Ion Beam Physics and Materials Research, Forschungszentrum Dresden-Rossendorf, P.O. Box 51 01 19, 01314 Dresden, Germany*

[2]*Institute of Radiochemistry, Forschungszentrum Dresden-Rossendorf, P.O. Box 51 01 19, 01314 Dresden, Germany*

(Received 7 August 2009; accepted 17 August 2009; published online 24 September 2009)

Using combined electroluminescence (EL) and photoluminescence (PL) studies we establish that the energy transfer process from the Er^{3+} to the Ge-related oxygen-deficiency centers (GeODCs) plays the key role in enhancing the 404 nm EL intensity in Ge-rich SiO_2. Er doping induced structural modification does not appear to be relevant, which is deduced from the 404 nm PL *quenching* with increasing Er concentration, implying a gradual loss of GeODCs. In contrast to PL, the 404 nm EL intensity *increases* by 0.3% Er doping followed by a gradual decrease in intensity for higher Er concentrations, which is described in terms of a competition between the energy transfer process and the gradual segregation of Er due to the destruction of GeODCs with Er doping. This fact is further discussed in the light of *ab initio* molecular orbital calculations. © *2009 American Institute of Physics*. [doi:10.1063/1.3225911]

I. INTRODUCTION

Coupling and energy transfer processes between optically[1] or electrically[2] excited semiconductor nanocrystals (NCs) and rare-earth ions in SiO_2 have been the subject of various scientific investigations from both basic research and technological standpoints. For instance, doping of Si-rich SiO_2 layers by Er and the corresponding energy transfer mechanism from optically excited Si nanostructure to the Er^{3+} ions have extensively been investigated to exploit the enhancement of the 1.53 μm Er emission[1,3,4] that coincides well with the maximum transparency window of the silica based optical fiber. Beside Si nanostructures, ion or electron irradiation induced point defects in SiO_2 have also been invoked.[5,6] In fact, defects ultimately control the electrical or optical response of semiconductor NCs in a SiO_2 matrix. The relative influence between the defects and Si nanostructures for exciting nearby Er^{3+} ions is found to be associated with the sample preparation methods, such as deposition[7,8] and ion beam implantation techniques.[5]

Now the question arises what will happen if Ge nanostructures are incorporated instead of Si. Although the magnetosputtered grown Ge-rich SiO_2 has shown a weak impact on Er photoluminescence (PL),[7] the contribution of the Ge-related oxygen-deficiency centers (GeODCs) for the emission of blue-violet light in SiO_2 was reported to be increased by introducing additional Er.[8] In fact, the latter one was discussed in terms of Er concentration (C_{Er}) dependent structural modification in Ge-rich SiO_2. On the other hand, we have recently demonstrated an increase in the blue-violet electroluminescence (EL) intensity from Ge-implanted metal-oxide semiconductor (MOS) structures codoped with Er at the expense of the 1.53 μm Er emission.[6] The observed characteristics are opposite to the phenomena commonly reported in case of optically pumped Er-doped Si-rich SiO_2 layers.[3,4] Hence, this mechanism is denoted as *inverse energy transfer* process.[6]

In this article, we have initially evaluated the C_{Er} dependency of the electrically driven inverse energy transfer process from the Er^{3+} to the GeODCs in Ge-rich Er-doped MOS light-emitting devices by comparing the corresponding PL results. To follow this fact, prior to examine the impact of Er doping, we verify the structure of GeODC and the corresponding 404 nm emission by *ab initio* calculations. Note that the 404 nm emission from GeODC relies on the optical or electrical excitation of the first singlet state (S_1) followed by the intersystem crossing to the first triplet state (T_1) and a radiative transition back to the ground singlet state (S_0).[5,6] We also show the origin of an Er-related defect, namely, $[(H_3SiO)_2Er]^-$ by substituting Ge in GeODC by Er at low C_{Er}, while the Er_2O_3 phase is more probable for higher C_{Er}.

II. EXPERIMENTAL

The standard MOS structure was fabricated by local oxidation of Si (LOCOS) technology with a 200 nm thick thermally grown SiO_2 layer on *n*-type Si(100) wafer. Initially, 130 keV Ge ions were implanted with a maximum concentration of 3.5% at the mean projected range (R_p) of ~112 nm as derived from the SRIM-2006 calculations.[9] The samples were subjected to furnace annealing for 60 min at 950 °C to produce Ge NCs. Subsequently, 250 keV Er ions were implanted within a range of 0.3%–1.4% at R_p ~115 nm followed by annealing at 900 °C for 30 min to remove implantation-induced defects and to activate Er^{3+} ions.[10] The Ge and Er concentrations were further verified by Rutherford backscattering spectroscopy measurements with a 1.4 MeV $^4He^+$ beam. A 100 nm thick silicon-oxynitride layer

a)Electronic mail: a.kanjilal@fzd.de.

 © 2009 American Institute of Physics

[This article is copyrighted as indicated in the article. Reuse of AIP content is subject to the terms at: http://scitation.aip.org/termsconditions. Downloaded to] IP: 131.217.6.8 On: Wed, 03 Sep 2014 10:25:56

was deposited on top of the LOCOS structure. Moreover, semitransparent indium tin oxide and aluminum contacts were sputter deposited on the front and rear surfaces, respectively. The top layer was further patterned by optical lithography to achieve arrays of circular electrodes (diameter of ~300 μm). Cross-sectional transmission-electron-microscopy (TEM) images were taken by an FEI Titan 80-300 S/TEM instrument operating at 300 keV. All the EL spectra were recorded at room temperature (RT) with constant current mode under forward bias conditions and with a monochromator in combination with a photomultiplier. To follow the C_{Er} dependent systematic change in density of the GeODCs, RT PL measurements were carried out using a pulsed laser (Minilite™ Continuum's Q-switched neodymium doped yttrium aluminum garnet laser system, 266 nm wavelength, 5 ns pulse width, and 10 Hz frequency) with an average power density of ~0.4 mW/mm^2 on the sample surface; the spectrum and the time-resolved PL experiments were monitored by a HORIBA Jobin-Yvon spectrometer (model iHR550) connected with a charge-coupled device camera detector.

III. RESULTS AND DISCUSSION

Initially the formation of Ge NCs was verified by high-resolution TEM (HRTEM) where the typical distribution of NCs with average sizes of ~6.1 nm is displayed in Fig. 1(a). In the following phases of Er doping [Figs. 1(b)–1(d)], Ge NCs were fragmented and amorphized with increasing C_{Er}; details of the C_{Er} dependent microstructural modification are given elsewhere.[11] In order to gain an in-depth understanding of the microstructure, complementary PL measurements have also been carried out since the GeODCs are very much sensitive to the ultraviolet (266 nm) excitation, leading to an emission of a 404 nm band associated with the $T_1 \rightarrow S_0$ transition.[5] It is found that the 266 nm wavelength is nonresonant to the Er^{3+} emission.[12] Moreover, the defect-related 404 nm PL is found to quench systematically with increasing C_{Er} [Fig. 2(a)]. Note that the recorded 404 nm PL quenching is also expected if the optically excited GeODCs take part in transferring energy to the nearby Er^{3+} ions. Since the estimated decay time τ_d (~58 μs) is found to be unaffected even after introducing additional Er [inset of Fig. 2(a)], it appears that the 404 nm PL is likely to be governed by the effective density of GeODC rather than the participation of such defects in transferring energy to the vicinal Er^{3+} ions. In a recent publication,[8] interestingly an increase in the blue-violet PL intensity was observed by introducing excess Er in Ge-rich SiO_2 layers where the observed phenomenon was discussed in the light of an Er induced structural modification in Ge-rich SiO_2. Clearly, this model cannot justify the observed PL quenching with increasing C_{Er}. By correlating the PL results [Fig. 2(a)] with corresponding microstructures (Fig. 1), we can conclude that the reduction in the effective density of GeODCs is mainly correlated with the gradual fragmentation and amorphization of Ge NCs with increasing C_{Er}, giving indirect evidence of the existence of active GeODCs at the NC/SiO_2 interface.

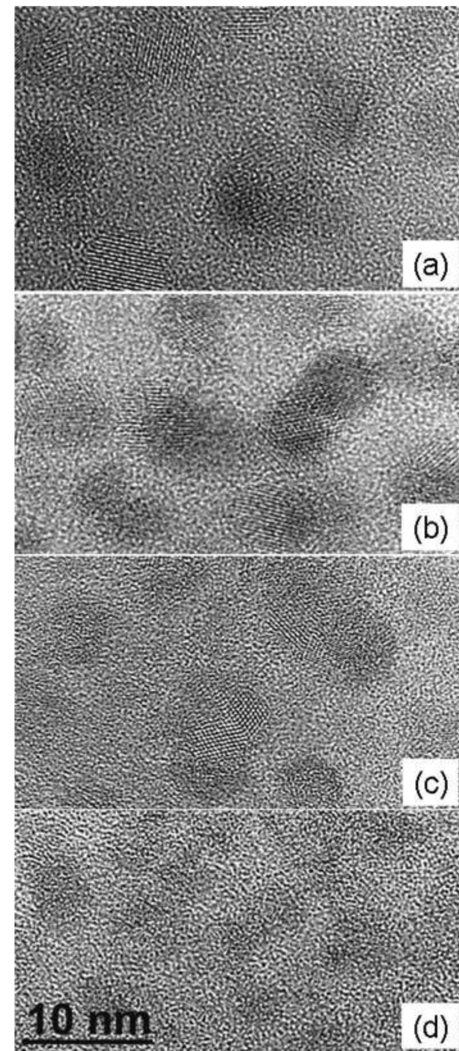

FIG. 1. The HRTEM images taken under similar magnification for only 3.5% Ge (a) and for 3.5% Ge with 0.3% Er (b), 0.8% Er (c), and 1.4% Er (d) in SiO_2.

To follow the impact of electrical excitation on the corresponding MOS structures, the EL spectra have also been recorded for a constant current density (J) of 1.4 mA/cm^2 [Fig. 2(b)]. Contrary to the PL results, a significant jump in 404 nm EL intensity is registered by introducing 0.3% Er, while it subsequently quenches with further Er doping. Clearly, C_{Er} determines the 404 nm EL intensity. We must note here that such an increase of the 404 nm EL intensity in Ge-rich MOS structures by Er doping has earlier been observed and explained in terms of an inverse energy transfer process.[6] Within this model, the energy is transferred from the higher energy states of the electrically excited Er^{3+} to the T_1 state of the adjacent GeODCs and subsequently relaxes down to the ground S_0 state by emitting light at ~404 nm. By comparing the PL and EL results, it seems that the gradual quenching of the 404 nm EL intensity above 0.3% Er [Fig. 2(b)] is associated with the overall reduction in density of GeODC with increasing C_{Er} [see Fig. 2(a)], suggesting a decrease in probability of the inverse energy transfer process during electrical pumping. Although the PL results confirm the destruction of a fraction of GeODCs even for a moderate Er doping (0.3%) [Fig. 2(a)], the corresponding EL spectrum

[This article is copyrighted as indicated in the article. Reuse of AIP content is subject to the terms at: http://scitation.aip.org/termsconditions. Downloaded to] IP: 131.217.6.8 On: Wed, 03 Sep 2014 10:25:56

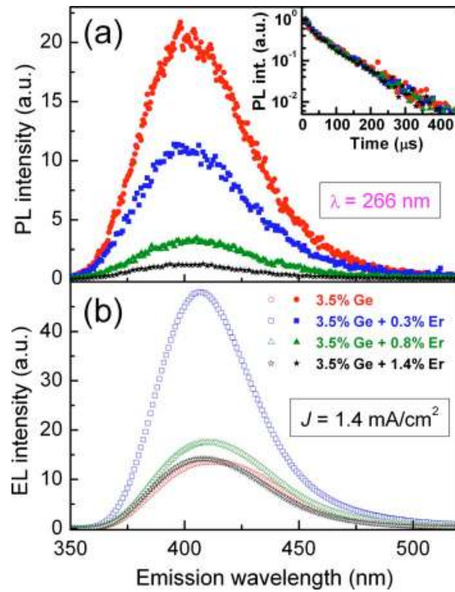

FIG. 2. (Color online) RT visible range PL spectra recorded after a delay time of 1 μs and plotted by *solid* symbols for only 3.5% Ge (circles) and for 3.5% Ge with 0.3% Er (squares), 0.8% Er (vertical triangles), and 1.4% Er (stars) in SiO_2 with an excitation wavelength of 266 nm are displayed in (a). The inset of (a) shows the PL decays for the corresponding structures at a wavelength of 404 nm. Similarly, the RT EL spectra for $J=1.4$ mA/cm^2 plotted by *open* symbols for only 3.5% Ge (circles) and for 3.5% Ge with 0.3% Er (squares), 0.8% Er (vertical triangles), and 1.4% Er (stars) in SiO_2 are exhibited in (b).

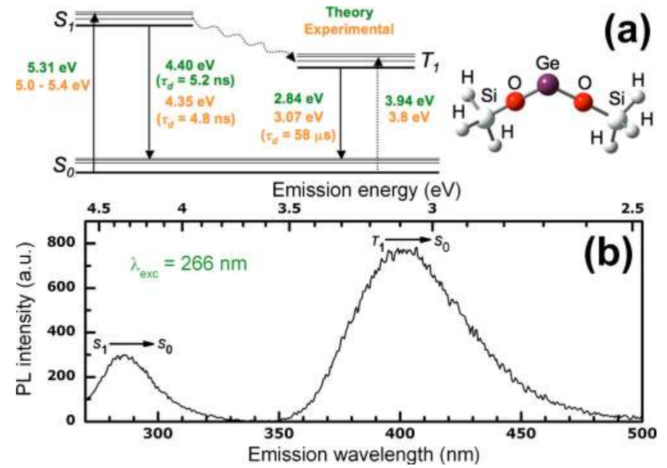

FIG. 3. (Color online) Energy level scheme of the GeODC, $(H_3SiO)_2Ge$, consisting of three energy states S_0, S_1, and T_1 with absorption and emission energies as well as calculated and experimentally determined lifetimes (a). A typical PL spectrum recorded after a delay time of 50 ns for only 3.5% Ge in SiO_2, showing $S_1 \rightarrow S_0$ and $T_1 \rightarrow S_0$ emission bands peaking at ~285 and 404 nm when excited by a wavelength of 266 nm (b).

[Fig. 2(b)] implies that the coupling between the remaining GeODCs with the Er^{3+} ions plays the pivotal role to initiate an energy transfer process from the Er^{3+} to GeODCs during electrical excitation. Owing to the destruction of more and more Ge-related defects with increasing C_{Er} [see Fig. 2(a)] the coupling between the Er^{3+} ions and GeODCs reduces markedly with gradual segregation of Er, resulting the formation of Er composites.[11,13]

To explore the interaction strength of the Er^{3+} with a localized GeODC and subsequent structural modification in Ge-rich SiO_2 with increasing Er doping more precisely, we performed *ab initio* molecular orbital (MO) calculations. First we have investigated the excitation and emission transitions in GeODCs and their oscillator strengths. For this, we considered the well studied defect structure $(H_3SiO)_2Ge$,[14] which acts like a molecule having three energetic states such as S_1, T_1, and S_0 [see Fig. 3(a)]. Geometry optimization of the $(H_3SiO)_2Ge$ cluster was performed at the complete active space self-consistent field (CASSCF) level with C_{2v} symmetry constraint for the three energy states S_0, S_1, and T_1. A single point energy calculation was performed by the second-order Møller–Plesset perturbation theory (MP2) using the CASSCF-optimized geometry. In the CASSCF calculations, four electrons were distributed among four active MOs, and all the electrons were correlated during the MP2 calculations. An all-electron triple-zeta plus polarization basis set was used on all atoms. Singlet-to-singlet ($S_0 \rightarrow S_1$) and singlet-to-triplet ($S_0 \rightarrow T_1$) excitations and the corresponding emissions were studied. The absorption and emission intensities were calculated by time-dependent Hartree–Fock (TD-HF) theory calculations. All the calculations were performed with GAUSSIAN 03 program packages.[15] The structural parameters such as Ge–O, Si–O distances, and O–Ge–O angles (estimated by means of CASSCF calculations) are found to be 1.75 Å, 1.67 Å, and 100° for S_0, 1.72 Å, 1.68 Å, and 114° for S_1, and 1.73 Å, 1.66 Å, and 115° for T_1, respectively.

Figure 3(a) shows the energy level scheme of GeODC where the transition energies obtained from both *ab initio* calculations and PL experiments are included. We find a good agreement between theoretical and experimental results. For example, the $S_1 \rightarrow S_0$ and $T_1 \rightarrow S_0$ emission bands were calculated to be 4.40 eV (282 nm) and 2.84 eV (437 nm), respectively, whereas the corresponding numbers obtained from our PL experiments are ~4.35 eV (~285 nm) and ~3.07 (~404 nm) eV [Fig. 3(b)]. Note that the extracted value for the $T_1 \rightarrow S_0$ emission (3.17 eV or 391 nm) is found to be close to the experimental value if we use time-dependent density functional theorem (TD-DFT) calculations. However, the TD-DFT calculation was not able to identify the geometry of the S_1 state and therefore, we used the CASSCF method, which gives geometries of all the states of interest. According to the MO analysis, the $S_0 \rightarrow T_1$ transition is mainly governed by the highest occupied molecular orbital (HOMO) to the lowest unoccupied molecular orbital (LUMO) transition, while both the HOMO and LUMO are centered on the Ge. Using TD-HF, the oscillator strength for the $S_1 \rightarrow S_0$ transition in gas phase is estimated to be 0.1788, which gives an emission lifetime of 5.2 ns, in agreement with the corresponding experimental value (4.8 ns). Since the triplet-to-singlet transition is spin forbidden, the TD-HF calculations give the oscillator strength of 0.0000, while the experimentally determined lifetime is found to be 58 μs that corresponds to the oscillator strength of 0.0001.

In order to theoretically interpret the effect of Er doping on the luminescence properties, we initially studied how the change in bulk properties affects the energy level and its intensity. The polarizable continuum model was used to mimic the surrounding bulk materials around GeODC, while

[This article is copyrighted as indicated in the article. Reuse of AIP content is subject to the terms at: http://scitation.aip.org/termsconditions. Downloaded to] IP: 131.217.6.8 On: Wed, 03 Sep 2014 10:25:56

the TD-HF calculations were performed to estimate the $S_1 \rightarrow S_0$ emission intensities. Using the permittivity of 3.8 for only SiO_2 we obtained an oscillator strength of 0.2004, while by using even a very high permittivity of 25.0, the oscillator strength only slightly increased to 0.2005. The change in bulk properties has only a negligible effect on the oscillator strength and therefore, the direct energy transfer from excited Er to the GeODC seems to be a more probable mechanism for the increase in the 404 nm EL intensity.

We substituted Ge in the GeODC by Er and calculated the structure of a $[(H_3SiO)_2Er]^-$ cluster at the MP2 level with C_{2v} symmetry constraint. The Er–O interatomic distance and the oxygen coordination number (CN) in $[(H_3SiO)_2Er]^-$ match well with those reported by Maurizio *et al.*[16] in low Er-doped Si-rich SiO_2 layers using extended x-ray absorption fine structure (EXAFS) spectroscopy. In particular, the Er–O distance determined from our calculation (using MP2) is found to be 2.01 Å, which is consistent with the value obtained from EXAFS (2.05 Å).[16] Moreover, the experimentally derived oxygen CN (3 ± 1) (Ref. 16) is found to be close to the theoretically obtained CN of 2 for the $[(H_3SiO)_2Er]^-$ cluster instead of 6 in the case of Er_2O_3. By increasing C_{Er}, Maurizio *et al.*[16] observed an increase in the Er–O interatomic distance to 2.27 Å and of CN to 6. It is reasonable to assume that in the course of Er doping in SiO_2 (and the same for Ge-rich SiO_2) initially formed $[(H_3SiO)_2Er]^-$ defects gradually switch to Er_2O_3, which is in good agreement with our x-ray diffraction results.[13] Concerning our spectroscopic results (Fig. 2), it seems that the Er atoms compete with the GeODCs where the local environments of Er, especially the first shell CN and the Er–O interatomic distance, play the crucial role for the 404 nm luminescence. Taking into account the optical properties (Fig. 2), our theoretical prediction establishes that the Er- and Ge-related defect centers cannot be isolated from each other—a prerequisite for the energy transfer process from the electrically excited Er^{3+} to the GeODCs, while the process is strongly affected due to the demolition of the GeODCs with the subsequent formation of Er composites with increasing C_{Er}, in good agreement with Ref. 13. Indeed, the present theoretical understanding allows us to follow the formation of the Er_2O_3 phase with gradual destruction of GeODCs with increasing C_{Er}, as derived from our PL studies [Fig. 2(a)]. However, the EL results [Fig. 2(b)] show how the inverse energy transfer process is affected with such gradual loss of GeODCs with increasing Er doping.

IV. CONCLUSIONS

In summary, comparing the PL properties we justify the energy transfer mechanism from the Er^{3+} to the nearest GeODCs during electrical pumping in Er-doped Ge-rich SiO_2 layers. In particular, we show an Er concentration dependent systematic degradation of the Ge-related defect centers by time and spectrally resolved PL experiments, exhibiting a quenching of the 404 nm PL without any change in decay time. We correlate the PL results with the corresponding EL and demonstrate that the overall energy transfer process from the Er^{3+} to the GeODCs is controlled by the Er-doping concentration. Our spectroscopic results verified by *ab initio* MO calculations give an evidence of the formation of a defect, namely, $[(H_3SiO)_2Er]^-$ cluster in SiO_2, which is expected to be formed by a close competition of Er with $(H_3SiO)_2Ge$ defect centers. Indeed, the theoretical approach highlights the Er concentration dependent gradual transformation of the $[(H_3SiO)_2Er]^-$ defect to Er_2O_3; this is in favor of the Er phase transformation observed in Ref. 13. The present empirical results are, therefore, reliable for explaining the Er concentration dependence of the inverse energy transfer process and thus the 404 nm EL intensity.

ACKNOWLEDGMENTS

We thank the Rossendorf Implantation Group for ion implantation and H. Felsmann, C. Neisser, and G. Schnabel for their careful semiconductor preparation work. This work is supported by the Alexander von Humboldt Foundation.

[1] A. Kanjilal, L. Rebohle, M. Voelskow, W. Skorupa, and M. Helm, J. Appl. Phys. **104**, 103522 (2008).
[2] F. Iacona, D. Pacifici, A. Irrera, M. Miritello, G. Franzò, F. Priolo, D. Sanfilippo, G. Di Stefano, and P. G. Fallica, Appl. Phys. Lett. **81**, 3242 (2002).
[3] B. Garrido, C. García, S.-Y. Seo, P. Pellegrino, D. Navarro-Urrios, N. Daldosso, L. Pavesi, F. Gourbilleau, and R. Rizk, Phys. Rev. B **76**, 245308 (2007).
[4] I. Izeddin, A. S. Moskalenko, I. N. Yassievich, M. Fujii, and T. Gregorkiewicz, Phys. Rev. Lett. **97**, 207401 (2006).
[5] L. Rebohle, J. von Borany, H. Fröb, and W. Skorupa, Appl. Phys. B: Lasers Opt. **71**, 131 (2000).
[6] A. Kanjilal, L. Rebohle, M. Voelskow, W. Skorupa, and M. Helm, Appl. Phys. Lett. **94**, 051903 (2009).
[7] C. L. Heng, T. G. Finstad, P. Storås, Y. J. Li, and A. E. Gunnæs, Appl. Phys. Lett. **85**, 4475 (2004).
[8] C. L. Heng, E. Chelomentsev, Z. L. Peng, P. Mascher, and P. J. Simpson, J. Appl. Phys. **105**, 014312 (2009).
[9] J. F. Ziegler, SRIM-2006.02 (http://www.srim.org).
[10] A. Janotta, M. Schmidt, R. Janssen, M. Stutzmann, and Ch. Buchal, Phys. Rev. B **68**, 165207 (2003).
[11] A. Kanjilal, L. Rebohle, M. Voelskow, W. Skorupa, and M. Helm, J. Appl. Phys. **106**, 026104 (2009).
[12] G. H. Dieke, *Spectra and Energy Levels of Rare Earth Ions in Crystals* (Interscience, New York, 1968), Chap. 13.
[13] A. Kanjilal, L. Rebohle, N. K. Baddela, S. Zhou, M. Voelskow, W. Skorupa, and M. Helm, Phys. Rev. B **79**, 161302(R) (2009).
[14] G. Pacchioni and R. Ferrario, Phys. Rev. B **58**, 6090 (1998).
[15] M. J. Frisch, G. W. Trucks, H. B. Schlegel, G. E. Scuseria, M. A. Robb, J. R. Cheeseman, Jr., J. A. Montgomery, T. Vreven, K. N. Kudin, J. C. Burant, J. M. Millam, S. S. Iyengar, J. Tomasi, V. Barone, B. Mennucci, M. Cossi, G. Scalmani, N. Rega, G. A. Petersson, H. Nakatsuji, M. Hada, M. Ehara, K. Toyota, R. Fukuda, J. Hasegawa, M. Ishida, T. Nakajima, Y. Honda, O. Kitao, H. Nakai, M. Klene, X. Li, J. E. Knox, H. P. Hratchian, J. B. Cross, V. Bakken, C. Adamo, J. Jaramillo, R. Gomperts, R. E. Stratmann, O. Yazyev, A. J. Austin, R. Cammi, C. Pomelli, J. W. Ochterski, P. Y. Ayala, K. Morokuma, G. A. Voth, P. Salvador, J. J. Dannenberg, V. G. Zakrzewski, S. Dapprich, A. D. Daniels, M. C. Strain, O. Farkas, D. K. Malick, A. D. Rabuck, K. Raghavachari, J. B. Foresman, J. V. Ortiz, Q. Cui, A. G. Baboul, S. Clifford, J. Cioslowski, B. B. Stefanov, G. Liu, A. Liashenko, P. Piskorz, I. Komaromi, R. L. Martin, D. J. Fox, T. Keith, M. A. Al-Laham, C. Y. Peng, A. Nanayakkara, M. Challacombe, P. M. W. Gill, B. Johnson, W. Chen, M. W. Wong, C. Gonzalez, and J. A. Pople, GAUSSIAN 03, Revision E.01, Gaussian, Inc., Wallingford, CT, 2004.
[16] C. Maurizio, F. Iacona, F. D'Acapito, G. Franzò, and F. Priolo, Phys. Rev. B **74**, 205428 (2006).

[This article is copyrighted as indicated in the article. Reuse of AIP content is subject to the terms at: http://scitation.aip.org/termsconditions. Downloaded to] IP: 131.217.6.8 On: Wed, 03 Sep 2014 10:25:56